RESEARCH ARTICLE

Troxerutin Induces Anticancer Efficacy in Human Hepatoblastoma Cell Line through G0/G1 Arrest and Mitochondria-Mediated Apoptosis

Nisha Susan Thomas,Nalini Namasivayam*

Department of Biochemistry and Biotechnology, Faculty of Science, Annamalai University, Tamil Nadu, India

ABSTRACT

Hepatoblastoma (HB) is the third most common abdominal neoplasm that occurs in children among the age group of 6 months-3 years. The present study was aimed to explore the anticancer efficacy of troxerutin (TX) on human colon hepatoblastoma cell line Hep G2. The cells were treated with different concentrations of TX (0.19-100 µM) to evaluate the effective IC_{50} dose at different time point 24 h, 48 h and 72 h. The effects of troxerutin on apoptotic morphology, mitochondrial membrane potential and on reactive oxygen species generation were examined by specific staining techniques in a time dependent manner (24 h and 48 h). The effect of TX on oxidative stress markers was determined by biochemical evaluation of antioxidants and lipid peroxidation profile and effect on DNA damage was determined by comet assay. Our results revealed that treatment with TX induced morphological changes and apoptotic characteristics including chromatin condensation, nuclear and DNA fragmentation in Hep G2 cells. Furthermore, our results revealed that treatment with TX induced mitochondrial membrane depolarization and significant ($p<0.05$) alterations in the oxidative stress markers (TBARS, SOD, CAT, GPx and GSH) as compared to the control untreated cells. Our findings conclude that TX significantly suppressed the cell viability and induced apoptosis in the Hep G2 cells in a dose and time dependent manner.

Keywords: Hepatoblastoma; Troxerutin; Oxidative stress; DNA fragmentation; Apoptosis.

INTRODUCTION

HB is the most common malignancy and the third most common abdominal neoplasm that occurs mainly in children among the age group of 6 months-3 years[1,2]. An increased incidence and risk of HB has been clinically reported in premature babies with less than 1 kilo of birth weight[3]. Based on the past 21-years of survey by the Surveillance, Epidemiology and End Results (SEER) program of the National Cancer Institute, HB accounts about 79 % of the childhood (under the age of 15) liver cancer[4]. The most common symptoms of HB are abdominal mass, abdominal discomfort, loss of appetite, fatigue, vomiting, peritoneal irritation and severe anemia. The current diagnostic modalities of HB are abdominal ultrasonography, computed tomography (CT) or magnetic resonance imaging (MRI). During the past decades clinical studies pointed out that the only complete surgical resection of the tumor are the successive curative method and the hope for long-term survival[4]. However, chemotherapy has proved to be effective in both adjuvant as well as neoadjuvant settings. The substitution of chemotherapy in the hepatoblastoma treatment emerged during the early 1970s. The practice of neoadjuvant chemotherapy has resulted in the resection of nonmetastatic hepatoblastomas with decreased morbidity of surgery. Even though the chemotherapeutic agents such as doxorubicin and cisplatin showed an effective chemopreventive effect over hepatoblastoma, those exerted potential side effects including cardiac toxicity and nephrotoxicity. Thus unfortunately, the outcome of the patients with nonresectable or recurrent disease still remains poor and new chemotherapeutic strategies and agents are needed [3].

The human hepatoblastoma cell line Hep G2 was originated and excised from the liver of 15 years old white male and established in 1979 by Barbara Knowles and collogues. The tumor is an exact example of an epithelial hepatoblastoma. The molecular characterization and gene

*Corresponding Author: Dr. Nalini Namasivayam**, Email:** nalininam@yahoo.com

expression profiling studies in the Hep G2 cells demonstrates the fetal and embryonal hepatoblastoma features[5].Hep G2 cell line is an excellent source for understanding the phenotypic and genotypic nature of hepatoblastoma and is the most commonly used cell line for hepatoblastoma chemotherapeutic research [6].

Troxerutin (TX), also known as vitamin P4 is a derivative of bioflavonoid rutin, hydroxyethylated ($–CH_2-CH_2-OH$) at 3', 4' and 7th positions on rutin skeleton. TX is mainly extracted from the flower buds of *Sophora japonica* (Japanese pagoda tree) and widely present in dietary elements like tea, coffee, cereal grains and a variety of fruits and vegetables. It has been extensively used for a number of therapeutic purposes including treatment of chronic venous insufficiency (CVI) and improving capillary function. TX also exhibited properties such as anti-thrombotic, fibrinolytic, antioxidant, anti-inflammatory, anti-diabetic, anti-cancer, odema-protective, neuro-protective, radioprotective and rheological activities. In elderly patients and pregnant women, its safety and effectiveness has been successfully proved without any side effects [7,8].

MATERIALS AND METHODS

Cell Culture and Treatments

Human hepatocarcinoma cell line Hep G2 (passage no: 15) was obtained from National Centre for Cell Science (NCCS), Pune, India and was maintained in Roswell Park Memorial Institute-1640 (RPMI-1640) medium supplemented with 10% fetal bovine serum (FBS) and 1% of 100 U/mL penicillin and 100 µg/mL streptomycin at 37°C in a humidified incubator with 5% CO_2.

Cell Viability Assay

The viability of Hep G2 cells were assessed by 3-(4,5-dimethylthiazol-2-yl)-2,5-diphenyl tetrazoli- um bromide (MTT) assay as described. Cells were treated with varying concentrations of TX (0.19-100 µM) for 24, 48 and 72 h. The optical density was measured at a wavelength of 570 nm, with a reference wavelength of 690 nm using a microtitre plate reader (BioRad). The experiments were performed as tetraplicate. Percentage of inhibition was calculated using the following formula:

$$Cell\ viability(\%) = \frac{[(Mean\ absorbance\ of\ control\ cells)-(Mean\ absorbance\ of\ the\ treated\ cells)]}{[(Mean\ absorbance\ of\ control\ cells)]} \times 100$$

Assessment of Nuclear Condensation

Characteristic apoptotic morphological changes induced by TX in Hep G2 cells were determined by acridine orange (AO) and ethidium bromide (EB) staining. In brief, Hep G2 cells were grown in 6-well plates (5×10^3 cells/well) for 24 h. The cells were then incubated with TX for 24 and 48 h, respectively. After incubation, medium was discarded and the cells were washed with phosphate buffered saline (PBS). The cells were then stained with AO/EB for 15 min at 37°C in dark and subsequently viewed in a fluorescence microscope (Carl Zeiss, Jena, Germany) with excitation wavelength 502 nm and emission wavelength 526 nm.

Hoechst 33258 Staining

The apoptotic morphological changes in TX treated and untreated Hep G2 cells were detected by staining trypsinized cells (5×10^5/ml) with 10 µg/ml of Hoechst 33258 for 10 min at 37°C. A drop of cell suspension was placed on a glass slide and a cover slip was laid over to reduce light diffraction. The morphological changes were observed using a fluorescence microscope (Carl Zeiss, Jena, Germany) fitted with a 377-355 nm filter and the cells reflecting apoptotic changes were observed and photographed.

Determination of reactive oxygen species (ROS) generation

Intracellular ROS generation was analyzed using the oxidation-sensitive fluorescent probe 2',7'–dichlorofluorescin diacetate (DCFH-DA), that measures the hydroxyl, peroxyl and other reactive oxygen species within the cell, as described by Murugan et al.[9]. After treatment of Hep G2 cells with TX for 24 h and 48 h, cells were rinsed with phosphate buffered saline and incubated with 10 µM DCFH-DA for 15 min at 37°C in dark. After diffusion of DCFH-DA, into the cell, it is deacetylated by cellular esterases to a non-fluorescent compound, which is further oxidized by ROS into 2',7'–dichlorofluorescein (DCF). The intensity of the highly fluorescent DCF was detected by fluorescence microscopy (Carl Zeiss, Jena, Germany) with maximum excitation and emission spectra of 495 nm and 529 nm respectively.

14

Determination of DNA damage

Microgel estimation of DNA strand break was measured by the method of Singh, 2000[10]. Frosted microscopic slides were covered with 200 µl of 1% normal melting agarose and above which the second layer of 100 µl of 1% low melting agarose containing approximately 10^5 cells was added. Cover slip was placed immediately and the slides were placed at 4°C. After solidification of the low melting agarose, the cover slip was removed and the slides were placed in the chilled lysis solution containing 2.5 M NaCl, 100 mM EDTA and 1% Triton X-100 for 16 h at 4°C. The slides were removed from the lysing solution and placed on a horizontal electrophoresis tank filled with freshly prepared alkaline buffer (300 mM NaOH, 1 mM EDTA, pH >13.00). The slides were equilibrated in the same buffer for 20 min and electrophoresis was carried out at 25 V, 180 mA for 20 min. After electrophoresis, the slides were washed gently with distilled water. The slides were then stained with 50 µl of ethidium bromide and visualized using a Nikon fluorescence microscope equipped with a 365 nm excitation filter and a 435 nm barrier filters.

Analysis of Mitochondrial Transmembrane Potential (ΔΨm)

The changes in the mitochondrial membrane potential were determined using mitochondria specific dye, rhodamine 123. Briefly, cells were seeded in a 6-well plate (5×10^3 cells/well) for 24 h. After 24 h and 48 h of treatment with TX, cells were incubated with 10 µl rhodamine 123 (1 mg/ml) for 30 min in dark at 37°C and was examined under a fluorescence microscope (Carl Zeiss, Jena, Germany).

Caspase-3 Activity Assay

Caspase-3 enzyme activity was assayed using Caspase-Glo3/7 reagent kit (Promega, Mumbai, India). Hep G2 cells (1×10^5 cells/well) grown in 96-well plates, were treated with TX and incubated at 37°C for 12 and 24 h. Subsequently, after incubation 100 µL of Caspase-Glo3/7 reagent was added to each well and mixed thoroughly using a plate shaker for 1 min. The plates were then incubated at room temperature for 2 h. Luminescence was measured using a microplate reader (Biorad680 XR) with the excitation and emission wavelengths set at 380 and 440 nm respectively.

Flow Cytometric Analysis

The cell cycle distribution in control and TX treated Hep G2 cells ($1x10^5$ cells) were analyzed using flow cytometry. After TX treatment for 24 and 48 h, cells were harvested, washed with phosphate-buffered saline (PBS), and fixed in 70% ethanol at 4°C for 2 h. The cells were then resuspended and incubated in PBS containing 1 mg/ml PI and 1 µl RNase and 10 µl Triton® X-100 for 1 h at 37°C in dark. The percentage of Hep G2 cells in different cell cycle phase were calculated using FACS DNA analysis software.

Scratch Wound Healing assay

Hep G2 cells were seeded (1×10^5 cells/well) in 6-well plates and then pre-incubated for 24 h in serum free RPMI-1640 before initiating a wound across the monolayer with a tip. After incubation, the serum free medium was replaced with complete medium and the cells were treated with TX. After 24 h and 48 h of incubation, the migration of cells into the wound surface was monitored by microscopy (Carl Zeiss, Jena, Germany).

Biochemical assessment of antioxidant enzyme activity and lipid peroxidation profile

Control and TX treated cells in T75 flask were trypsinized and washed with PBS. The harvested cells were suspended in 10 µM dithiothreitol, 130 mM KCl and 50 mM PBS and vortexed briefly. The cells were then centrifuged at 10,000 rpm at 4°C for 10 min and the resulting supernatant was used for biochemical estimations. The level of lipid peroxidation byproduct, thiobarbituric acid reactive substances (TBARS) in HuH-7 was determined by the method of Niehaus and Samuelson [11]. The activities of enzymic and non-enzymic antioxidants such as superoxide dismutase (SOD), catalase (CAT), glutathione (GSH) and glutathione peroxidase (GPx) were assayed by the method of Kakkar et al.[12], Sinha[13], Ellman [14] and Rotruck et al.[15] respectively.

RESULTS

Effect of troxerutin on cell viability:

To determine the effect of TX on Hep G2 cell viability, the cells were treated with increasing concentrations of TX for 24, 48 and 72 h. The cytotoxicity assay showed that TX significantly reduced the Hep G2 cell viability in a

dose- and time-dependent manner (**Fig.1A**) with IC_{50} values of 3.02 µM, 1.35 µM and 0.78 µM at 24, 48 and 72 h, respectively. Thus, TX showed growth-inhibitory effects on human hepatic cancer cell line Hep G2.
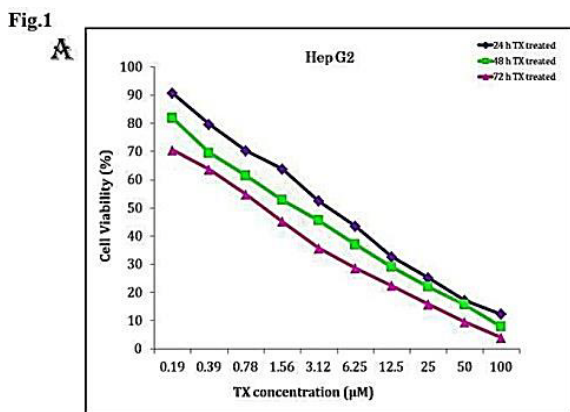

Fig 1: A- Effect of troxerutin on cell viability (MTT assay) in Hep G2 cells. The cells were treated with different concentrations of troxerutin (0.19-100 µM), which decreased the cell viability in a time dependent manner 24h 48 h and 72 h respectively. Data are expressed as mean ± SD of three independent experiments.

Effect of troxerutin on cellular morphology reflecting apoptotic features:

The morphological changes in Hep G2 cells revealed inhibition of cell growth and induction of cell death after treatment with TX for 24 and 48 h. TX treated cells exhibited characteristics such as formation of plasma membrane blebs, cell shrinkage, loss of membrane integrity, reduction in cell volume, impaction of cells and dissembled gaps between neighboring cells and the remaining adherent cells, confirming the occurrence of apoptosis. The untreated control cells formed a monolayer with high confluency as compared to TX treated cells as shown in (**Fig.1B**).
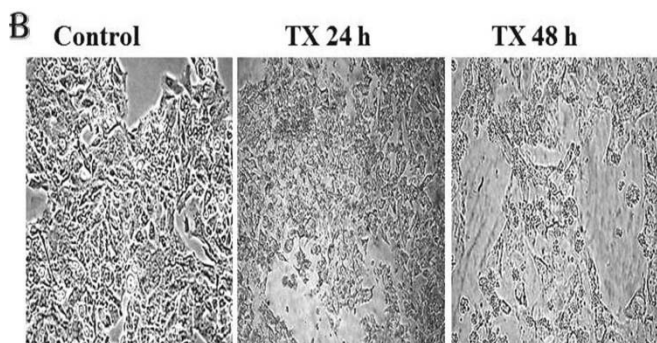

Fig 1: B- Effect of troxerutin on the cell morphology of Hep G2 cells. Control cells showing well defined cellular morphology. Troxerutin treated (24 h and 48 h) cells showing cell shrinkage, plasma membrane blebbing, and loss of cell membrane integrity.

The cytotoxic potential and apoptotic efficacy of TX in Hep G2 cells was further confirmed with acridine orange/ethidium bromide (AO/EB) and Hoechst 33258 fluorescence staining as shown in (**Fig2 A& B**).AO/EB dual staining in TX treated Hep G2 cells showed time-dependent increase in chromatin condensation (a hallmark of apoptosis) as compared to the control untreated cells. In dual staining, AO stained both viable cells and fragmented nuclei green where the fragmented green nucleus indicates early apoptotic cells whereas EB selectively stained the cell nuclei yellowish green indicating late apoptosis.The cells treated with TX for 24 and 48 h, showed signs of early apoptosis (Fig.2 ATX 24h and TX 48h) as compared to untreated control cells in which the nuclei as well as cytoplasm revealed uniform green fluorescence.
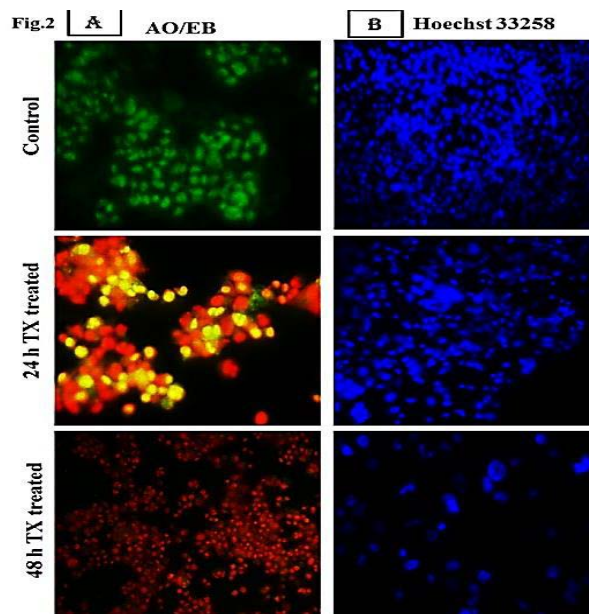

Fig 2: A- Effect of troxerutin on the cell morphology of Hep G2, AO/EB stained. Control cells showed viable cells with uniform green fluorescence. 24 h and 48 h troxerutin treated cells showing chromatin condensation indicating early and late apoptotic cells emitting uniform bright yellowish green and red fluorescence. **B-** Effect of troxerutin on nuclear morphology oh Hep G2 cells (Hoechst 33258 staining). Control cells showed normal nuclei. 24 h and 48 h troxerutin treated cells showing nuclear swelling, condensed chromatin, fragmented nuclei and apoptotic bodies.

The TX treated and untreated cells were further stained with Hoechst 33258 stain to observe the apoptotic nuclear morphology. Many cells among the TX treated group showed nuclear shrinkage, fragmented nuclei and apoptotic bodies, indicating the apoptotic efficacy of TX in a time dependent manner as compared to the

control untreated cells (Fig.2B TX 24h and TX 48h). These data clearly reveals that TX induces marked changes in the cellular morphology thus decreasing the cell viability immensely.

The results of DNA fragmentation assay also affirmed the apoptotic effect of TX in Hep G2 cells. Treatment with TX in a time dependent manner caused acute DNA damage in Hep G2 cells, which was revealed by the appearance of comet with tail whereas in control, the cells were round and the DNA was observed to be intact. Comparatively, 48 h TX treated cells showed more prominent comet tail as compared to the DNA of 24 h treated cells. The difference in the DNA of the control and TX treated cells were viewed under a fluorescence microscope as represented in (Fig3B).
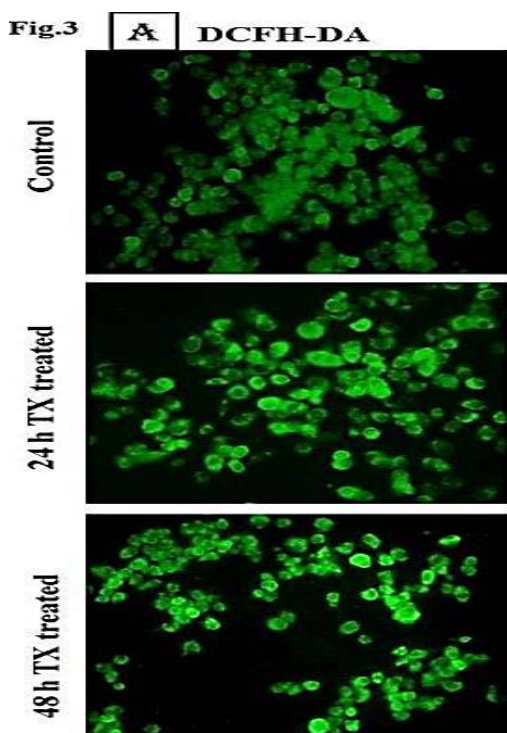

Fig 3: A-Effect of troxerutin on ROS generation in control and troxerutin treated Hep G2 cells. Control cells showing reduced content of ROS emitting minimal green fluorescence. Troxerutin treated (24 h and 48 h) cells showing high content of ROS exhibiting bright green fluorescence.

Effect of troxerutin on the generation of intracellular reactive oxygen species (ROS):

TX treated Hep G2 cells, exhibited a bright green fluorescence indicating significantincrease in the intracellular ROS whereas the control untreated cells exhibited only minimal green fluorescence (**Fig3A**).This clearly

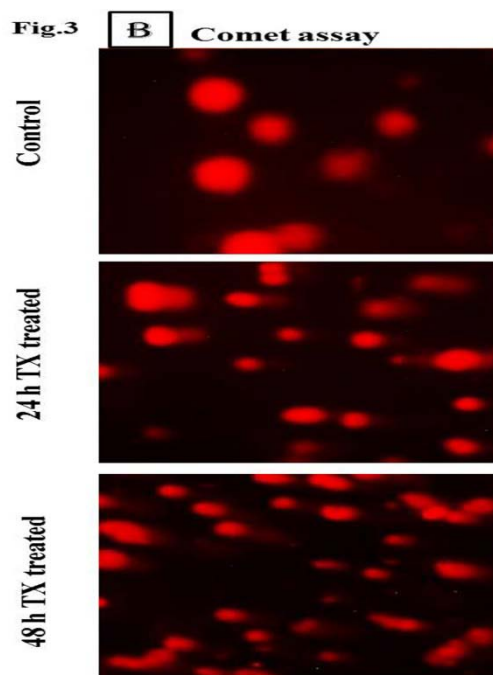indicates that TX generates ROS in Hep G2 cells and thereby induces ROS mediated apoptosis.

Fig 3: B- Effect of troxerutin on DNA damage in Hep G2 cells (comet assay). Control cells showed round intact nucleus. 24 h and 48 h troxerutin treated cells showing comet like DNA tail.

Effect of troxerutin on membrane potential of mitochondria (ΔΨm) and caspase-3 activation:

The mode of apoptosis induced by TX was determined by analyzing ΔΨm, which is a reliable quantification of mitochondria-dependent apoptosis. The effect of TX on ΔΨm was analyzed using the mitochondrion-specific dye rhodamine123. The untreated control cells with high ΔΨm expressed intense green fluorescence whereas treatment of the cells with TX for 24 h and 48 h induced a significant reduction in ΔΨm (mitochondrial transmembrane depolarization), expressing diminished green fluorescent apoptotic cells (Fig. 4A), indicating that TX induces mitochondria-dependent apoptosis, which may be due to caspase-3 activation. Caspase-3 activity was assayed fluorimetrically and the results showed 2.5 and 3.2 fold increase in caspase-3 activation at 24 h and 48 h TX treatment as compared to the control untreated cells (Fig.4B), affirming that TX induces mitochondria-dependent apoptosis in Hep G2 cells.
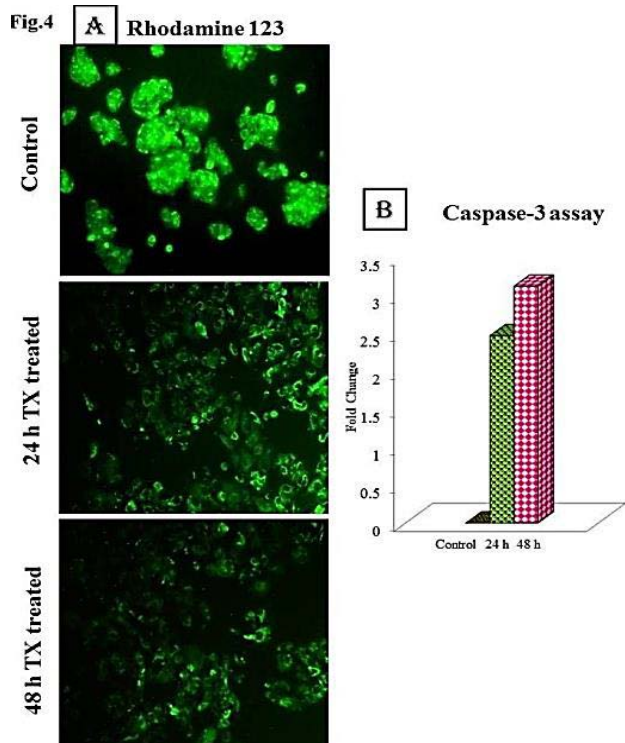
Fig 4: A- Effect of troxerutin on the mitochondrial membrane potential (ΔΨm) in Hep G2 cells (rhodamine 123 stained). Control cells shows intense green fluorescence indicating high mitochondrial membrane potential. Troxerutin treated (24 h and 48 h) cells shows weak green fluorescence due to mitochondrial membrane depolarization. **B-**Expression of cleaved caspase 3 in Hep G2 cells treated with troxerutin at 24 h and 48 h. Control cell shows no expression of caspase-3. 24 h and 48 h troxerutin treated cells shows increased levels of caspase-3 expression.

Effect of troxerutin on cell cycle progression:

To determine whether TX exhibited its anti-cancer activity through perturbation of cell cycle in Hep G2 cells, cell cycle analysis was performed. Flow cytometric analysis profile revealed that treatment of Hep G2 cell with TX in a time-dependent manner (24 and 48 h) resulted in Hep G2 cell proliferation arrest in G1/G0 phase of the cell cycle and decreased the proportion of cells in the S-phase (**Fig5A**). In both 24 h and 48 h time period, the proportion of Hep G2 cells in G2/M phase of the cell cycle remained nearly the same. Thus, the result indicates that TX inhibits cell proliferation exhibiting its anti-proliferative efficacy.

Effect of troxerutin on cell migration:

Scratch wound migration assay was performed to investigate the inhibitory effect of TX on the migration potency of Hep G2 cells. As shown in (**Fig 5B**), migration of TX treated Hep G2 cells (24 and 48h) were significantly reduced

and/or inhibited into the wounded area, which was analyzed by the movement of cells into the wound as compared to control untreated cells. The effect of TX was more pronounced in 48 h treatment. The result showed that TX inhibited the motility of Hep G2 cells exhibiting its anti-migratory potential.
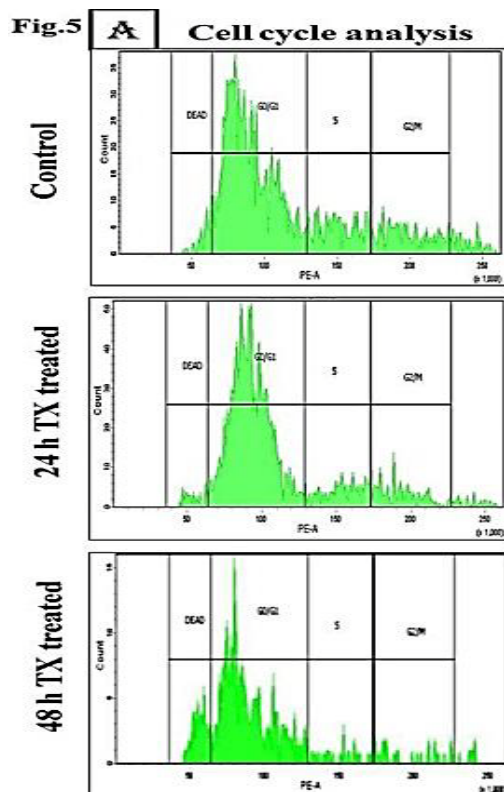

Fig 5: A- Flow cytometric analysis in Hep G2 cells. Control cells showing cells in progressive cell cycle phases and reduced cell death. Hep G2 cells treated with IC$_{50}$ concentration of TX for 24 and 48 h, stained with propidium iodide showing cell cycle arrest at G0/G1 phase, reduced number of cells in S and G2/M2 phase of the cell cycle and increased number of cell death.

Effect of TX on lipid peroxidation profile and antioxidant enzyme activities

Treatment of Hep G2 cells with TX showed a significant increase in the level of TBARS and significant decrease in the activities of enzymic and non-enzymic antioxidants such as SOD, CAT, GSH and GPx as compared to the control untreated cells (table 1), revealing the pro-oxidative role of TX in HuH-7 cells.

DISCUSSION

Determining the underlying mechanism by which a compound inhibits abnormal cell growth, cell proliferation and induces cell death, enables the development of novel chemotherapeutic agents with less side effects[16]. In this study, the

cytotoxic effect of TX was examined on HB cell line Hep G2 at different concentrations (0.19-100 μM) and at different time points 24 h, 48 h and 72 h respectively. It was observed that the IC$_{50}$ concentration of TX was 3.02 μM at 24 h. TX inhibited the HB cell growth to a wide extent in a linear and time-dependent manner. The cytotoxic effect of TX on HB was similar to that of other flavonoids such as naringenin, rutin and quercetin on Hep G2 cells as reported in the previous studies[17-20].

Fig 5: B- Migration assay in Hep G2 cells. Control cells show vigorous migration towards the wound area. Troxerutin treated (24 h and 48 h) cells shows reduced migration across the wounded area.

Apoptosis is an essential mechanism to maintain the homeostatic balance in normal cells. Numerous pre-clinical studies have pointed out various anti-cancer polyphenolic compounds including curcumin, ellagic acid, apigenin, chrysin, EGCG, resveratrol, quercetin and silymarin that targets the apoptotic signaling pathway directly and/or indirectly. Targeting an apoptotic pathway and shedding light on its molecular mechanisms has provided great evidences for novel anti-cancer drug development.[21,22,23] In the present study, treatment of Hep G2 with specific IC$_{50}$ dose of TX at different time points (24 h and 48 h), induced apoptotic morphological characteristics such as cell shrinkage, loss of membrane integrity,

reduced cellular volume, chromatin condensation, internucleosomal DNA degradation and reduced the number of live cells. Large number of apoptotic cells was observed when the cell lines were treated with TX for prolonged time period i.e., 48 h as compared to the 24 h treatment revealing that the mode of cell death induced by TX was apoptosis besides necrosis which could be attributed to the free radicle scavenging and proapoptotic properties of TX. The hydroxyl group in TX might be the reason for the selective cytotoxicity of TX to the HB cells.
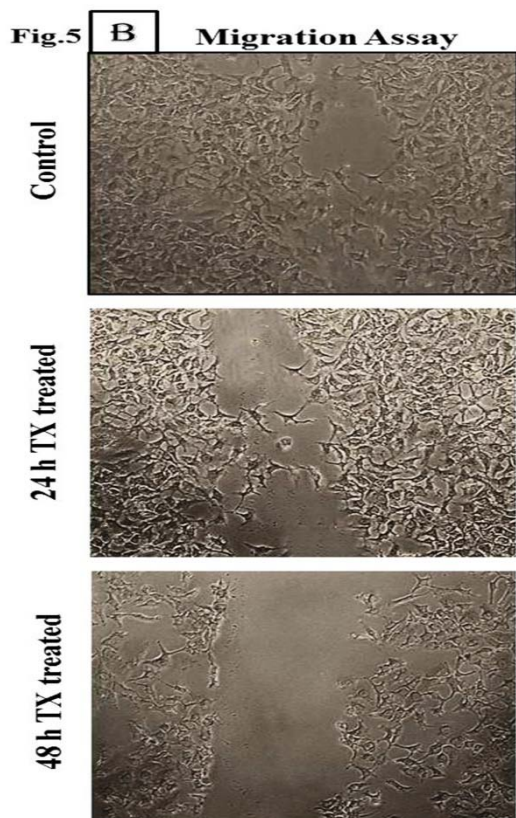
Mitochondria are the main source of the signals that regulates apoptotic cell death and it contains the key regulators of caspase that are apoptotic factors. Mitochondrial membrane potential is considered as a major indicator of the apoptotic cell fate. The opening of mitochondrial permeability transition pore induces the mitochondrial transmembrane depolarization (ΔΨm), thereby releasing the apoptogenic factors and leading to the loss of oxidative phosphorylation.[24,25,26] In the present study, the TX treated Hep G2 cells showed mitochondrial membrane depolarization revealing mitochondria mediated apoptotic cell death in Hep G2 cells. This effect of TX might be due to the ability of TX to elevate ATP production or exert mitochondrial dysfunction. ROS generation is known to be a crucial factor and play a vital role in regulation of cellular processes such as intracellular signaling, metabolism, cell proliferation and apoptosis. The level of ROS in the cells under normal cellular circumstances is well balanced by the antioxidants such as SOD, CAT, and GSH but upon cellular injury this balance is disrupted altering the cellular defense mechanism. Recent studies have been focusing on selective killing of cancer cells by enhancing the ROS levels in cancer cells to a higher level thus directly triggering the ROS accumulation or inhibiting the ROS scavenging systems in the cell.[27,28] In the present study, TX treatment increased the ROS generation in Hep G2 cells, which could be due to the pro-oxidative potential of TX in HB cells. The pro-oxidative nature of TX also reduced oxidative stress, exposing Hep G2 cells to endogenously produced ROS, affirming the role of ROS in TX induced apoptosis.

Table 1: Effect of troxerutin on TBARS and antioxidant enzymes

Cell line	Hep G2		
Groups	Control	24 h TX treated	48 h TX treated
TBARS[♥]	6.14 ± 0.13^a	13.94 ± 0.94^b	14.68 ± 1.23^c
SOD[♠]	12.41 ± 1.30^a	9.06 ± 1.08^b	8.52 ± 0.80^c
CAT[♣]	7.57 ± 0.79^a	5.52 ± 0.47^b	3.84 ± 0.42^c
GPx[♦]	4.78 ± 0.68^a	3.87 ± 0.70^b	2.72 ± 0.54^c
GSH[§]	10.83 ± 1.1^a	8.12 ± 0.80^b	6.33 ± 0.60^c

[♥]mmoles/ml of cell lysate; [♠] 50% NBT reduction/min/mg protein; [♣]µmoles of H_2O_2 utilized/min/mg protein; [♦]µmoles of GSH utilized/min/mg protein; [§]mmole/mg tissue protein. Data are presented as the means ± SD of four independent experiments in each group. Values not sharing a common superscript letter ([a-c]) differ significantly at p<0.05 (DMRT).

G1 and G2 phases of the cell cycle are considered as the major check points and are known to plays a vital role in cell cycle progression. Thus regulation of these cell cycle proteins could probably inhibit and/or restrict repeated cancer cell proliferation.[29,30] In the present study TX exerts its antitumor activity and apoptotic effects by causing cell cycle arrest at the G0/G1 phase of cell cycle. The above results reveal that TX induced apoptosis in the HB cell line Hep G2, markedly by inhibiting the cell viability, cell migration and by inducing DNA fragmentation.

Overall, TX demonstrated significant anticancer, antiproliferative and anti-migratory activities in HB cell line by causing pronounced apoptotic morphological changes, generation of ROS, cell cycle regulatory effects, decreased mitochondrial membrane potential and activation of Casp-3. The anticancer activity of TX *in vitro* might be due to the activation and cleavage of apoptotic gene Casp-3.

ACKNOWLEDGEMENT

REFERENCE
1. Chattopadhyay S, Mukherjee S, Boler A, Sharma A, Biswas SK. Hepatoblastoma in the neonatal period: An unusual presentation. J Cytol. 2012; 29: 252-4.
2. Moon SB, Shin HB, Seo JM, Lee Sk. Hepatoblastoma: 15-years experience and role of surgical treatment. J Korean Surg Soc. 2011; 81: 134-40.
3. Hiyama E. Pediatric hepatoblastoma: diagnosis and treatment. TranslPediatr. 2014; 3: 293-9.
4. Herzog EC, Andrassy RJ, Eftekhari F. Childhood cancers: Hepatoblastoma. The Oncologist. 2002; 5: 445-453.
5. Lopez-Terrada D, Cheung SW, Finegold MJ, Knowles BB. Hep G2 is a hepatoblastoma-derived cell line. Hum Pathol. 2009; 40: 1512-5.
6. Syam S, Abdul AB, Sukari MA, Mohan S, Abdelwahab SI, Wah TS. The growth suppressing effects of girinimbine on Hep G2 involve induction of apoptosis and cell cycle arrest. Molecules. 2011; 16: 7155-7170
7. Panat NA, Singh BG, Maurya DK, Sandur SK, Ghaskadbi SS. Troxerutin, a natural flavonoid binds to DNA minor groove and enhances cancer cell killing in response to radiation. ChemBiol Interact. 2016; 251: 34-44.
8. Thomas NS, George K, Arivalagan S, Mani V, Siddique Al, Namasivayam N. The in vivo antineoplastic and therapeutic efficacy of troxerutin on rat preneoplastic liver: biochemical, histological and cellular aspects. Eur J Nutr. 2016; [Epub ahead of prnt].
9. Murugan RS, Priyadarsini RV, Ramalingam K, Hara Y, Karunagaran D, Nagini S. Intrinsic apoptosis and NF-kB signaling are potential molecular targets for chemoprevention by black tea polyphenols in HepG2 cells in vitro and in a rat hepatocarcinogenesis model in vivo. Food Chem. Toxicol. 2010: 48; 3281–3287.
10. Singh NP. Microgels for estimation of DNA strand break DNA protein crosslink and apoptosis. Mutat Res. 2000; 455: 111-112.
11. Niehaus WG, Samuelson B. Formation of malondialdehyde from phospholipid arachidonate during microsomal lipid peroxidation. Eur J Biochem. 1968; 6;126-130.
12. Kakkar PS, Das B, Viswanathan P. A

20

modified spectrophotometeric assay for superoxide dismutase. Indian J. Biochem. Biophys. 1984; 21:130–132.

13. Sinha AK. Colorimetric assay of catalase. Anal. Biochem. 1972; 47:389–394.

14. Ellman GL. Tissue sulphydryl groups. Arch. Biochem. Biophys. 1959; 82:70–77.

15. Rotruck JT, Pope AL, Ganther HE, Swanson AB, Hafeman DG, Hoekstra WG. Selenium: biochemical role as acomponent of glutathione peroxidase. Science. 1973; 179:588–590.

16. Souza AO, Pereira LC, Oliveira DP, Dorta DJ. BDE-99 congener induces cell death by apoptosis of human hepatoblastoma cell line – HepG2. Toxicol in vitro. 2013; 27: 580-587

17. Yen HR, Liu CJ, Yeh CC. Naringenin suppresses TPA-induced tumor invasion by suppressing multiple signal transduction pathways in human hepatoblastoma and hepatocellular carcinoma cells. ChemBiol Interact. 2015; 235:1-9.

18. Vrba J, Kren V, Vacek J, Papouskova B, Ulrichova J. Quercetin, quercetin glycosides and taxifolin differ in their ability to induce AhR activation and CYP1A1 expression in HepG2 cells. PhytotherRes. 2012; 26: 1746-52.

19. Kozics K, Valovicova Z, Salmenova D. Structure of flavonoids influences the degree inhibition of Benzo(a)pyrene - induced DNA damage and micronuclei in HepG2 cells.Neoplasma. 2011; 58: 516-24.

20. Barcelos GR, Grotto D, Angeli JP, Serpeloni JM, Rocha BA, Bastos JK, Barbosa F. Evaluation of antigenotoxic effects of plant flavonoids quercetin and rutin on HepG2 cells. Phytother Res. 2011; 25: 1381-8.

21. Ramos S. Cancer chemoprevention and chemotherapy: dietary polyphenols and signalling pathways. Mol Nutr Food Res. 2008; 52: 507-26.

22. Hongmei Z. Extrinsic and intrinsic apoptosis signal pathway review. T. Ntuli (Ed.). Apoptosis and Medicine, InTech. 2012

23. Yeh CT, Yen GC. Effect of sulforaphane on metallothionein expression and induction of apoptosis in human hepatoma HepG2 cells.Carcinogenesis. 2005; 26: 2138-48.

24. Logan A, Pell VR, Shaffer KJ, Evans C, Stanley NJ, Robb EL, Prime TA, Chouchani ET, Cocheme HM, Fearnley IM, Vidoni S, James AM, Porteous CM, Partridge L, Kreq T, Smith RA, Murphy MP.Assessing the mitochondrial membrane potential in cells and *in vivo* using targeted click chemistry and mass spectrometry. Cell Metab. 2016; 23: 379-85.

25. Ly JD, Grubb DR, Lawen A.The mitochondrial membrane potential ($\Delta\Psi$m) in apoptosis; an update. Apoptosis. 2003; 8:115-28.

26. Gottlieb E, Armour SM, Harris MH, Thompson CB. Mitochondrial membrane potential regulates matrix configuration and cytochrome c release during apoptosis.Cell Death Differ. 2003; 10: 709-17.

27. Nogueira V and Hay N. Molecular pathways: reactive oxygen species homeostasis in cancer cells and implications for cancer therapy. Clin Cancer Res. 2013; 19: 4309-14.

28. Sullivan LB, Chandel NS. Mitochondrial reactive oxygen species and cancer. Cancer Metab. 2014; 2: 17.

29. Sherr CJ. Cancer cell cycles. Science. 1996; 274:1672-7.

30. CollinsK, Jacks T, Pavletich NP. The cell cycle andcancer. PNAS.1997; 94: 2776 - 2778.